KIAS-P15052

arXiv:1509.07410v3 [hep-ph] 11 Jan 2016

Leptoquark explanation of $h \to \mu\tau$ and muon $(g-2)$

Seungwon Baek[1, *] and Kenji Nishiwaki[1, †]

[1] *School of Physics, KIAS, 85 Hoegiro, Seoul 02455, Korea*

We consider lepton flavor violating Higgs decay, specifically $h \to \mu\tau$, in a leptoquark model. We introduce two scalar leptoquarks with the $SU(3)_c \times SU(2)_L \times U(1)_Y$ quantum numbers, $(3, 2, 7/6)$ and $(3, 2, 1/6)$, which do not generate dimension-4 operators mediating proton decay. They can mix with each other by interactions with the standard model Higgs. The constraint from the charged lepton flavor violating process, $\tau^- \to \mu^-\gamma$, is very strong when only one leptoquark contribution is considered. However, we demonstrate that significant cancellation is possible between the two leptoquark contributions. We show that we can explain the CMS (ATLAS) excess in $h \to \mu\tau$. We also show that muon $(g-2)$ anomaly can also be accommodated.

PACS numbers: 12.60.Fr, 12.60.-i, 13.85.Qk

---

[*] Electronic address: swbaek@kias.re.kr

[†] Electronic address: nishiken@kias.re.kr

I. INTRODUCTION

Leptoquarks (LQs) are scalar particles which carry both baryon and lepton numbers [1]. They appear in gauge theories with "unified" gauge groups, such as Pati-Salam model, $SU(5)$ grand unification, etc.

Since LQs are strongly interacting particles which can decay semileptonically, their masses are strongly bounded by the LHC experiments, such as ATLAS and CMS. For the third-generation scalar LQs, the ATLAS group excludes the mass in the range $m_{\rm LQ} < 625\,{\rm GeV}$ and $200\,{\rm GeV} < m_{\rm LQ} < 640\,{\rm GeV}$ at 95% confidence level (C.L.) based on their 8 TeV data, assuming 100% branching fractions into $b\nu_\tau$ and $t\nu_\tau$, respectively [2]. On the other hand, the CMS group had reported various 8 TeV bounds at 95% C.L. on $m_{\rm LQ}$ as $m_{\rm LQ} > 740\,{\rm GeV}$, $m_{\rm LQ} > 650\,{\rm GeV}$ and $m_{\rm LQ} > 685\,{\rm GeV}$ with assumptions of 100% branching fractions into $b\tau$, $t\nu_\tau$ and $t\tau$, respectively [3, 4].

We note that the CMS excess of $eejj$ and $e\nu jj$ [5] can also be interpreted as a signal of the first generation LQ with mass about 650 GeV. An example of detailed study of LQ models for the excess can be found in [6].

In the standard model (SM), lepton flavor violating (LFV) Higgs decay channels are absent at tree level and highly suppressed by small neutrino masses and the GIM mechanism at loop level. Therefore, once they are observed with sizable branching fractions, they indicate a clear signal of new physics beyond the SM. The CMS collaboration reported the LFV Higgs decay branching fraction, using the 19.7 fb^{-1} of $\sqrt{s} = 8$ TeV,

$$\mathcal{B}(h \to \mu\tau) = (0.84^{+0.39}_{-0.37})\%, \tag{I.1}$$

which deviates 2.4σ from zero [7]. Here, $\mu\tau$ means the inclusive final state consisting of $\mu^+\tau^-$ and $\mu^-\tau^+$. Although recent ATLAS measurement, using the 20.3 fb^{-1} of $\sqrt{s} = 8$ TeV,

$$\mathcal{B}(h \to \mu\tau) = (0.77 \pm 0.62)\%, \tag{I.2}$$

does not show a significant deviation from the SM [8], it is at least consistent with the CMS result. If confirmed by the future data at LHC Run II which can probe down to $\sim 10^{-3}$, it would be a clear signal requiring new physics beyond the SM. There are several model-independent [9–21] and also model-dependent studies [22–38] to accommodate this deviation.

The theoretical and experimental sensitivity of the anomalous magnetic moment of the muon, *i.e.* $(g-2)_\mu$, has reached to probe the electroweak scale. State of the art calculations in the SM cannot explain the experimental result, and there is about 3σ discrepancies between them [39, 40]:

$$\Delta a_\mu = a_\mu^{\rm exp} - a_\mu^{\rm SM} = (299 \pm 90 \;\; \text{to} \;\; 394 \pm 84) \times 10^{-11}, \tag{I.3}$$

which also calls for new physics models.

In this paper we consider a LQ model as an explanation of the LFV Higgs decay, $h \to \mu\tau$ and muon $(g-2)$ anomaly. Considering the proton decay constraints, only two types of $SU(2)_L$ doublet leptoquarks are favored. We assume both of them are realized in nature. We first show that a strong constraint from $\tau^- \to \mu^-\gamma$ can be alleviated significantly due to cancellations between the top and bottom quark contributions.[1] We show that there is allowed parameter space to accommodate the $h \to \mu\tau$ anomaly and $(g-2)_\mu$. A smoking gun signal which distinguishes our model from other models would be the direct LQ production at colliders. A promising signature at the LHC is the pair production of LQs decaying into a quark and a lepton, where the decay pattern is so characteristic. Especially, components with $+2/3$ electric charge, named as Y_1 and Y_2 later, should be relatively light and couple to the bottom quark, the electron and the muon for the explanation of the excess in $h \to \mu\tau$ and the muon $(g-2)$ with circumventing the bound from $\tau^- \to \mu^-\gamma$. Therefore, the smoking gun final states in our model are $b\overline{b}\,\tau^-\tau^+$ and $b\overline{b}\,\mu^-\mu^+$.

The paper is organized as follows. In Sec. II, we introduce our model. In Sec. III, we consider $\tau^- \to \mu^-\gamma$ constraint. In Sec. IV, we consider $h \to \mu\tau$ signal. In Sec. V, we show that we show that we can accommodate $(g-2)_\mu$. In Sec. VI, we summarize and conclude.

II. THE MODEL

Among the possible LQs which have renormalizable interactions with the SM fermions, only R_2 and $\widetilde{R}_2$ in the notation of [1] do not have problem with the constraint from the proton decay within renormalizable perturbation theory [6, 41]. They are in the representation

$$R_2(3, 2, 7/6), \quad \widetilde{R}_2(3, 2, 1/6), \tag{II.1}$$

---

[1] Note that similar discussions in the context of LQs are found in [30, 36].

in the SM gauge group $SU(3)_C \times SU(2)_L \times U(1)_Y$.[2]

Assuming both of them exist in nature at renormalizable level, they interact with quarks and leptons via the interaction Lagrangian

$$\mathcal{L} \;=\; -\lambda_u^{ij}\overline{u}_R^i R_2^T \epsilon\, L_L^j - \lambda_e^{ij}\overline{e}_R^i R_2^\dagger Q_L^j - \lambda_d^{ij}\overline{d}_R^i \widetilde{R}_2^T \epsilon\, L_L^j + h.c., \tag{II.2}$$

where we have suppressed color indices and ϵ ($\equiv i\sigma^2$) is the two-by-two antisymmetric matrix with $\epsilon^{12} = 1$. The scalar potential is given by

$$\begin{aligned} V \;=&\; \mu_H^2|H|^2 + \mu_2^2|R_2|^2 + \widetilde{\mu}_2^2|\widetilde{R}_2|^2 \\ &+\; \lambda_H|H|^4 + \lambda_2|R_2|^4 + \widetilde{\lambda}_2|\widetilde{R}_2|^4 + \lambda_{HR}|H|^2|R_2|^2 + \widetilde{\lambda}_{HR}|H|^2|\widetilde{R}_2|^2 \\ &+\; \lambda_{H2}R_2^\dagger H H^\dagger R_2 + \widetilde{\lambda}_{H2}\widetilde{R}_2^\dagger H H^\dagger \widetilde{R}_2 + \left(\lambda_{\rm mix}R_2^\dagger H \widetilde{R}_2 \epsilon\, H + h.c.\right), \end{aligned} \tag{II.3}$$

where $H(1,2,1/2)$ is the SM Higgs doublet. R_2 and $\widetilde{R}_2$ fields can be decomposed into $SU(2)_L$ components,

$$R_2 = \begin{pmatrix} V \\ Y \end{pmatrix}, \quad \widetilde{R}_2 = \begin{pmatrix} \widetilde{Y} \\ \widetilde{Z} \end{pmatrix}. \tag{II.4}$$

After the Higgs gets vacuum expectation value (vev), $v\,(\simeq 246\,\text{GeV})$, we can write

$$H = \begin{pmatrix} 0 \\ \frac{1}{\sqrt{2}}(v+h) \end{pmatrix}, \tag{II.5}$$

in the unitary gauge. Then, the masses of V and $\widetilde{Z}$ are given by

$$m_V^2 = \mu_2^2 + \frac{1}{2}\lambda_{HR}v^2, \quad m_{\widetilde{Z}}^2 = \widetilde{\mu}_2^2 + \frac{1}{2}\widetilde{\lambda}_{HR}v^2 + \frac{1}{2}\widetilde{\lambda}_{H2}v^2. \tag{II.6}$$

The mass terms of Y and $\widetilde{Y}$ are written as

$$\mathcal{L}_{\rm mass}(Y,\widetilde{Y}) = -\begin{pmatrix} Y^\dagger & \widetilde{Y}^\dagger \end{pmatrix} \begin{pmatrix} \mu_2^2 + \frac{1}{2}\lambda_{HR}v^2 + \frac{1}{2}\lambda_{H2}v^2 & \frac{1}{2}\lambda_{\rm mix}v^2 \\ \frac{1}{2}\lambda_{\rm mix}v^2 & \widetilde{\mu}_2^2 + \frac{1}{2}\widetilde{\lambda}_{HR}v^2 \end{pmatrix} \begin{pmatrix} Y \\ \widetilde{Y} \end{pmatrix}. \tag{II.7}$$

---

[2] In the case of non-$SU(2)_L$-doublet LQs, we can write down gauge-invariant dimension-four operators generating rapid proton decay. The $SU(2)_L$ doublet ones do not allow such dangerous operators at renormalizable level. However, as discussed in [6, 41], constraints from dimension-five effective operators (generating proton decay) are still severe, where $m_{\rm LQ}$ should be greater than around 10^5 TeV even when the cutoff scale is equal to the Planck scale. A remedy for reducing $m_{\rm LQ}$ is to introduce a new symmetry prohibiting the operators. In this paper, we do not consider constraints from the proton decay caused by higher dimensional operators.

The mass eigenstates, Y_1, Y_2 (with the electromagnetic charge $+2/3$) are mixture of Y and $\widetilde{Y}$ with mixing angle α_Y,

$$\begin{pmatrix} Y \\ \widetilde{Y} \end{pmatrix} = \begin{pmatrix} c_Y & s_Y \\ -s_Y & c_Y \end{pmatrix} \begin{pmatrix} Y_1 \\ Y_2 \end{pmatrix} \equiv O \begin{pmatrix} Y_1 \\ Y_2 \end{pmatrix}, \tag{II.8}$$

where $c_Y = \cos\alpha_Y, s_Y = \sin\alpha_Y$.

As we will see, large α_Y and large mass splitting between V and Y_i are favored to satisfy the experimental constraints and also to enhance $h \to \mu\tau$. Concretely speaking, the relation $m_{Y_i} \sim m_V/6$ will be imposed to avoid the bound from $\tau^- \to \mu^-\gamma$ naturally with sizable couplings, which are required for explanations of the excess in $h \to \mu\tau$.

Here, we look into the mass matrix in Eq. (II.7) and discuss whether we can realize the mass hierarchy as $m_{Y_i} \sim m_V/6$ with a large mixing in α_Y in our setup. A key point is that the $(1,1)$ component of the mass matrix is rephrased as $m_V^2 + \frac{1}{2}\lambda_{H2}v^2$. Then, when the following relations are realized,

$$m_V^2,\ \lambda_{H2}v^2\ >\ \lambda_{\text{mix}}v^2,\ \widetilde{\mu}_2^2 + \frac{1}{2}\widetilde{\lambda}_{HR}v^2, \tag{II.9}$$

and a cancellation occurs between m_V^2 and $\frac{1}{2}\lambda_{H2}v^2$ with a negative λ_{H2}, the relation $m_{Y_i} \sim m_V/6\,(i = 1,2)$ can be realized. In addition, if the off-diagonal terms are comparable with diagonal ones, a large mixing angle in α_Y is expected. For example, if the (1,1) and (2,2) components are of similar size with $\sim \mathcal{O}(1)$ TeV^2 and $\lambda_{\text{mix}} \sim 10$, we get $m_{Y_{1,2}} \gtrsim 0.7$ TeV and a maximal α_Y, which can obviously avoid the current direct search bound on third generation LQs. However, when m_V is multi TeV, a realization of such cancellation between m_V^2 and $\frac{1}{2}\lambda_{H2}v^2$ would get to be nontrivial within perturbative λ_{H2}. To further enhance mass difference between V and Y_i and/or the mixing angle α_Y, we can implicitly assume additional contributions via higher dimensional operators such as

$$\frac{\phi}{\Lambda}R_2^\dagger H H^\dagger R_2, \quad \frac{\phi}{\Lambda}R_2^\dagger H \widetilde{R}_2 \epsilon\, H, \tag{II.10}$$

where ϕ is a new singlet with a large vev as $\langle\phi\rangle > \Lambda$.

Although there is no apparent symmetry which leads to the mass ratio $m_{Y_i} \sim m_V/6$, the UV complete grand unified theory (GUT) or flavor theory into which our low energy effective theory is embedded have larger symmetry and we expect they guarantee the mass ratio without fine tuning. The high energy theory will also generate the dimension-five operators in (II.10).

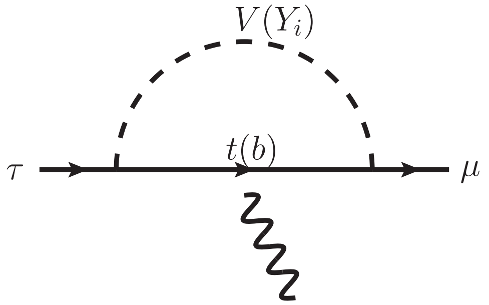

FIG. 1: Feynman diagrams for $\tau^- \to \mu^-\gamma$. The photon line can be attached to any charged particles, and there are four possibilities.

Finally, we comment on the case with a small mixing angle α_Y, which corresponds to the possibility that no sizable cancellation occurs between the terms m_V^2 and $\frac{1}{2}\lambda_{H2}v^2$. Even in this case, (at least) one mass eigenstate can be light as the relation $m_{Y_i} \sim m_V/6$ being fulfilled. But, as we will see in Sec. III, we should accept a larger hierarchy between two leptoquark couplings to circumvent the bound from $\tau^- \to \mu^-\gamma$. To make matters worse, as discussed in Sec. IV, such hierarchical couplings are inappropriate for explaining the excess in $h \to \mu\tau$.

III. $\tau^- \to \mu^-\gamma$

In this section, we consider the constraints from the charged lepton flavor violating processes. Since we are interested in $2 \leftrightarrow 3$ transitions, we restrict ourselves only to $\tau^- \to \mu^-\gamma$ decay. Our study can be applied to other LFVs, such as $\mu^- \to e^-$ or $\tau^- \to e^-$ transitions, similarly. However, we assume they are sufficiently suppressed by small LFV couplings.

The effective Hamiltonian for $\tau^- \to \mu^-\gamma$ is written as

$$\mathcal{H}_{\rm eff} = C_R^\gamma\, \overline{\mu}_L \sigma^{\mu\nu} F_{\mu\nu} \tau_R + C_L^\gamma\, \overline{\mu}_R \sigma^{\mu\nu} F_{\mu\nu} \tau_L, \tag{III.1}$$

where $C_{R,L}^\gamma$ are Wilson coefficients and $F_{\mu\nu}\,(= \partial_\mu A_\nu - \partial_\nu A_\mu)$ is the photon field strength tensor.

The Feynman diagrams for $\tau^- \to \mu^-\gamma$ are shown in Fig. 1. We note that in our model, the chirality flip appearing in (III.1) can occur inside the loop. Therefore the amplitudes can be proportional to m_t or m_b instead of small masses from the external lines, m_τ or m_μ. This is the main reason that this LFV process becomes a very strong constraint in ordinary third generation LQ models.

The Wilson coefficients $C^{\gamma}_{R,L}$ can be calculated from the diagrams in Fig. 1:

$$\begin{aligned}
C^{\gamma}_{R} &= \frac{N_c e}{32\pi^2 m_V^2}\left[\Big(\lambda_e^{23}\lambda_e^{33*}m_\mu + \lambda_u^{32*}\lambda_u^{33}m_\tau\Big)\Big(\frac{2}{3}I_1(x)+\frac{5}{3}J_1(x)\Big) + \lambda_u^{32*}\lambda_e^{33*}m_t\Big(\frac{2}{3}I_2(x)+\frac{5}{3}J_2(x)\Big)\right] \\
&+ \sum_{j=1,2}\frac{N_c e}{32\pi^2 m_{Y_j}^2}\left[\Big(\lambda_e^{23}\lambda_e^{33*}O_{1j}^2 m_\mu + \lambda_d^{32*}\lambda_d^{33}O_{2j}^2 m_\tau\Big)\Big(-\frac{1}{3}I_1(y_j)+\frac{2}{3}J_1(y_j)\Big)\right. \\
&+ \left.\lambda_d^{32*}\lambda_e^{33*}O_{1j}O_{2j}m_b\Big(-\frac{1}{3}I_2(y_j)+\frac{2}{3}J_2(y_j)\Big)\right], \\
C^{\gamma}_{L} &= \frac{N_c e}{32\pi^2 m_V^2}\left[\Big(\lambda_u^{32*}\lambda_u^{33}m_\mu + \lambda_e^{23}\lambda_e^{33*}m_\tau\Big)\Big(\frac{2}{3}I_1(x)+\frac{5}{3}J_1(x)\Big) + \lambda_e^{23}\lambda_u^{33}m_t\Big(\frac{2}{3}I_2(x)+\frac{5}{3}J_2(x)\Big)\right] \\
&+ \sum_{j=1,2}\frac{N_c e}{32\pi^2 m_{Y_j}^2}\left[\Big(\lambda_d^{32*}\lambda_d^{33}O_{2j}^2 m_\mu + \lambda_e^{23}\lambda_e^{33*}O_{1j}^2 m_\tau\Big)\Big(-\frac{1}{3}I_1(y_j)+\frac{2}{3}J_1(y_j)\Big)\right. \\
&+ \left.\lambda_e^{23}\lambda_d^{33}O_{1j}O_{2j}m_b\Big(-\frac{1}{3}I_2(y_j)+\frac{2}{3}J_2(y_j)\Big)\right], \qquad \text{(III.2)}
\end{aligned}$$

where $N_c = 3$ is the color factor, $x = m_t^2/m_V^2$, and $y_i = m_b^2/m_{Y_i}^2$. The loop functions are obtained to be

$$\begin{aligned}
I_1(x) &= \frac{2+3x-6x^2+x^3+6x\log x}{12(1-x)^4}, \\
J_1(x) &= \frac{1-6x+3x^2+2x^3-6x^2\log x}{12(1-x)^4}, \\
I_2(x) &= \frac{-3+4x-x^2-2\log x}{2(1-x)^3}, \\
J_2(x) &= \frac{1-x^2+2x\log x}{2(1-x)^3}. \qquad \text{(III.3)}
\end{aligned}$$

The branching ratio of $\tau^- \to \mu^-\gamma$ is then

$$\mathcal{B}(\tau^- \to \mu^-\gamma) = \frac{\tau_\tau (m_\tau^2 - m_\mu^2)^3}{4\pi m_\tau^3}\left(|C^{\gamma}_{R}|^2 + |C^{\gamma}_{L}|^2\right), \qquad \text{(III.4)}$$

where $\tau_\tau = 87.03\ \mu\text{m}$ is the lifetime of τ. The current experimental bound is [42]

$$\mathcal{B}(\tau^- \to \mu^-\gamma) < 4.4 \times 10^{-8}. \qquad \text{(III.5)}$$

This corresponds to

$$|C^{\gamma}_{R}|^2 + |C^{\gamma}_{L}|^2 < \left(\frac{4.75\times 10^{-10}}{\text{GeV}}\right)^2. \qquad \text{(III.6)}$$

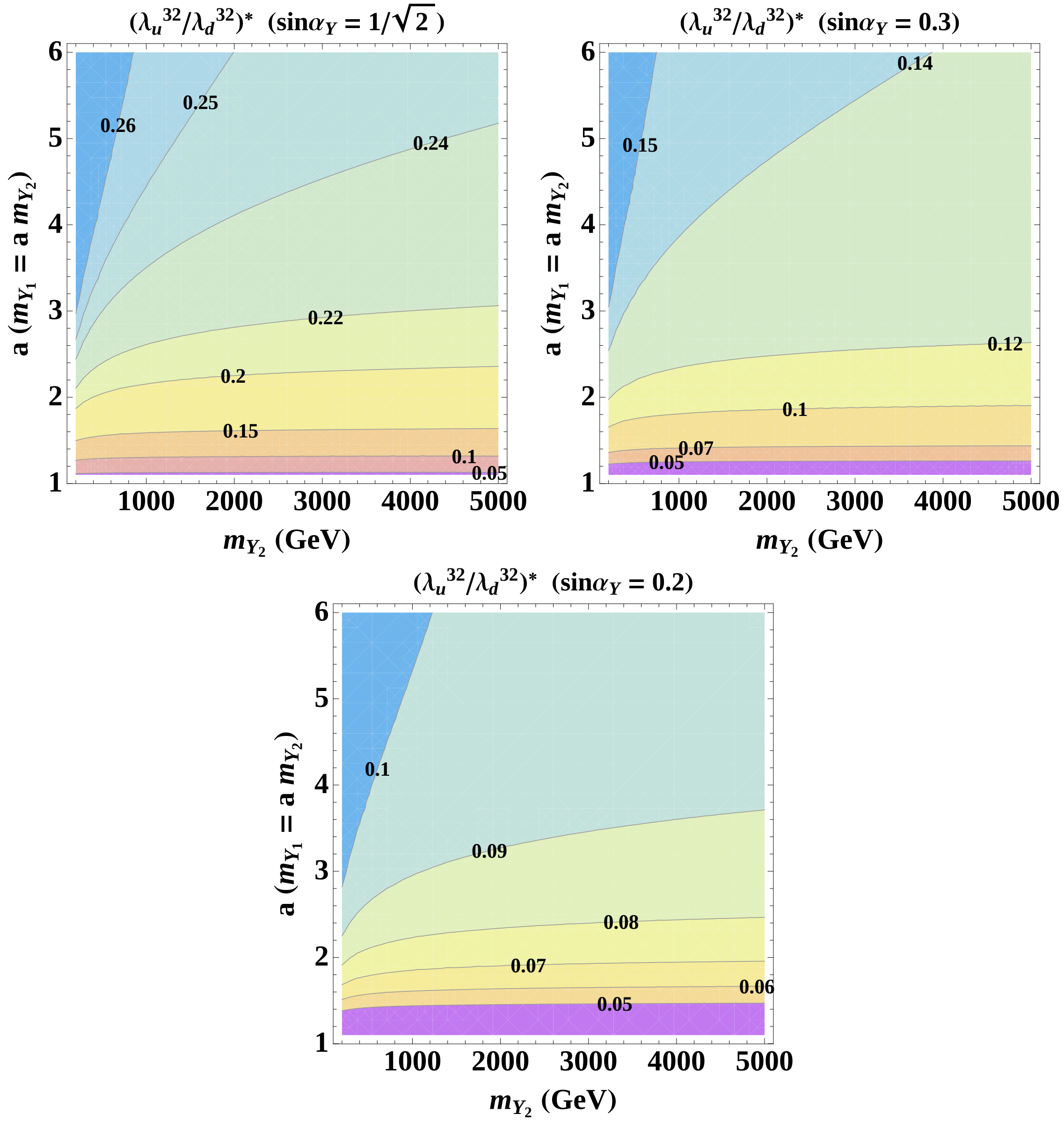

FIG. 2: Contour plots for $(\lambda_u^{32}/\lambda_d^{32})^*$ which is required for exact cancellations of $\tau^- \to \mu^-\gamma$ in (m_{Y_2}, m_{Y_1})-plane through Eq. (III.7). From top-left to bottom, the sine of the mixing angle $\sin\alpha_Y$ is chosen as $1/\sqrt{2}$, 0.3 and 0.2, respectively. m_V is set as $m_V = 6\, m_{Y_2}$ and m_{Y_1} is formulated as $m_{Y_1} = a\, m_{Y_2}$ by use of the factor a, where the range $[1.1, 6.0]$ is considered in the three plots.

For the discussion of $\tau^- \to \mu^-\gamma$, we assume $C_L^\gamma = 0$ for simplicity. If we consider a single leptoquark contribution from V, $\mathcal{B}(\tau^- \to \mu^-\gamma)$ gives lower mass bound $0.85, 3.7, 14, 42$ TeV, for $\lambda_e^{33} = 0.001, 0.01, 0.1, 1$, respectively, where we took $\lambda_u^{32} = 0.35$. With these parameters, we obtain too small contribution to $h \to \mu\tau$ as was noticed in [30].

Since we introduce both R_2 and $\widetilde{R}_2$, we can have diagrams with the chirality flip inside the b-quark loop, which generate terms proportional to m_b. The $Y_i - b$ contributions are naively expected to be smaller than $V - t$ contribution by factor $m_b/m_t \sim 1/35$. However, since $C^\gamma_{R,L}$ are proportional to $m_f/m^2_{\rm LQ}$ ($f = t, b$) as can be seen in (III.2), if $m_{Y_i} \sim m_V/6$, cancellations between t and b contributions can occur naturally. Note that a nonzero mixing between Y and $\widetilde{Y}$ is mandatory for a natural cancellation since in the limit $\sin\alpha_Y \to 0$ the contributions being proportional to m_b turn out to be zero. Neglecting small terms proportional to m_τ or m_μ, an exact cancellation in C^γ_R occurs when the following condition is held,

$$\frac{\lambda^{32*}_u}{\lambda^{32*}_d} = -\sum_{i=1}^{2} O_{1i}O_{2i}\,\frac{m_b}{m_t}\left(\frac{m_V}{m_{Y_i}}\right)^2 \frac{-\frac{1}{3}I_2(y_i) + \frac{2}{3}J_2(y_i)}{+\frac{2}{3}I_2(x) + \frac{5}{3}J_2(x)}. \tag{III.7}$$

In Fig. 2, the values of the ratio $(\lambda^{32}_u/\lambda^{32}_d)^*$ which are required for exact cancellations of $\tau^- \to \mu^-\gamma$ are shown as (m_{Y_2}, m_{Y_1})-planes through Eq. (III.7) with the three choices of the sine of the mixing angle $\sin\alpha_Y$ as $1/\sqrt{2}$, 0.3 and 0.2.[3] Here, m_V is set as $m_V = 6\, m_{Y_2}$ and m_{Y_1} is formulated as $m_{Y_1} = a\, m_{Y_2}$ by use of the factor a, where the range $[1.1, 6.0]$ is considered in the three plots. Note that in the case that m_{Y_1} and m_{Y_2} are completely degenerated, the two contributions being proportional to m_b are exactly canceled out between them and no cancellation mechanism works in $\tau^- \to \mu^-\gamma$. Here, almost all the shown regions in Fig. 2 (where $\sin\alpha_Y$ is greater than 0.2), the target values of the ratio $(\lambda^{32}_u/\lambda^{32}_d)^*$ are greater than 0.05, which means that we can adjust naturally the two couplings for realizing the cancellation. However, as we will see in the following section, when the ratio $(\lambda^{32}_u/\lambda^{32}_d)^*$ gets to be small, it is hard to explain the excess of $h \to \mu\tau$.

The Wilson coefficient C^γ_R can be rewritten in terms of the ratio in (III.7), which we will define as $(\lambda^{32*}_u/\lambda^{32*}_d)_{\rm cancel}$,

$$C^\gamma_R \simeq \frac{N_c e}{32\pi^2 m_V^2}\lambda^{32*}_u\lambda^{33*}_e m_t\Big(\frac{2}{3}I_2(x) + \frac{5}{3}J_2(x)\Big)\left[1 - \frac{\lambda^{32*}_d}{\lambda^{32*}_u}\left(\frac{\lambda^{32*}_u}{\lambda^{32*}_d}\right)_{\rm cancel}\right]. \tag{III.8}$$

This equation shows again that, if $\lambda^{32*}_d/\lambda^{32*}_u = (\lambda^{32*}_d/\lambda^{32*}_u)_{\rm cancel}$, $C^\gamma_R = 0$. We can consider a deviation from the exact cancellation by introducing δ in such a way that $\lambda^{32*}_d/\lambda^{32*}_u = (\lambda^{32*}_d/\lambda^{32*}_u)_{\rm cancel}(1 - \delta)$. Then we can take δ as a degree of required tuning for cancellation

---

[3] Note that the sign of $\sin\alpha_Y$ is not important. We can compensate a negative sign by flipping the sign of the coupling λ^{32}_u or λ^{32}_d.

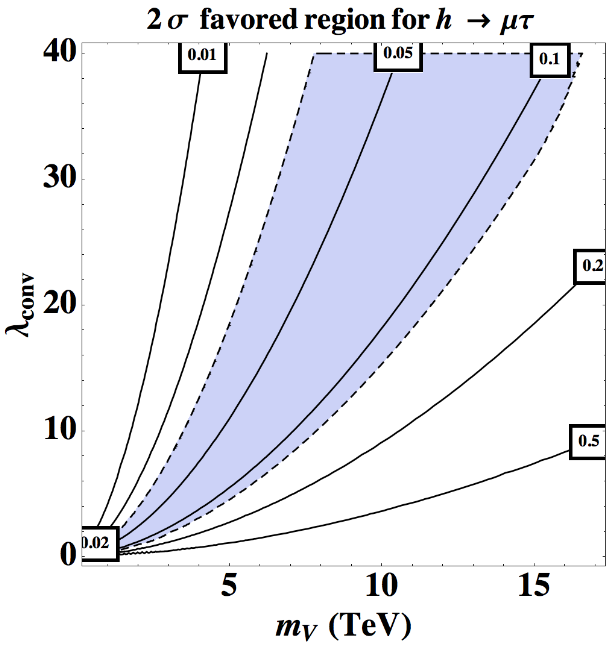

FIG. 3: The blue region shows the 2σ favored region for $h \to \mu\tau$ in $(m_V, \lambda_{\rm conv})$-plane, where $\lambda_{\rm conv} \equiv |\lambda_u^{32}\lambda_e^{33}|$. The black contours indicate degrees of the fine tuning defined around Eq. (III.8) in percentage terms.

in $\tau^- \to \mu^-\gamma$. In Fig. 3, the black lines show a constant contour plot of δ in $(m_V, \lambda_{\rm conv}(\equiv |\lambda_u^{32}\lambda_e^{33}|))$-plane in percentage terms when we take the upper limit on C_R^γ (with $C_L^\gamma = 0$) in Eq. (III.6). The plot shows that we need fine-tuning at the level of 0.1% to explain the excess of $h \to \mu\tau$ consistently.

IV. $h \to \mu\tau$

The lepton flavor violating Higgs decay is evaluated from the Feynman diagrams shown in Fig. 4. The divergence in diagram Fig. 4 (a) cancels those in Fig. 4 (c), (d), and the total result is finite, generating the dimension-four effective operators

$$\mathcal{H}_{\rm eff}(h \to \mu\tau) \;=\; h\overline{\mu}(C_R P_R + C_L P_L)\tau + H.c. \tag{IV.1}$$

The dimensionless effective couplings $C_{R,L}$ are calculated to be

$$C_R \;=\; -\lambda_u^{32*}\lambda_e^{33*}\frac{N_c m_t}{16\pi^2 v}\left[I_{acd}(r_t, r_h) + I_a(r_t, r_h) - \lambda_{HR}\frac{v^2}{m_V^2}I_b(r_t, r_h)\right]$$

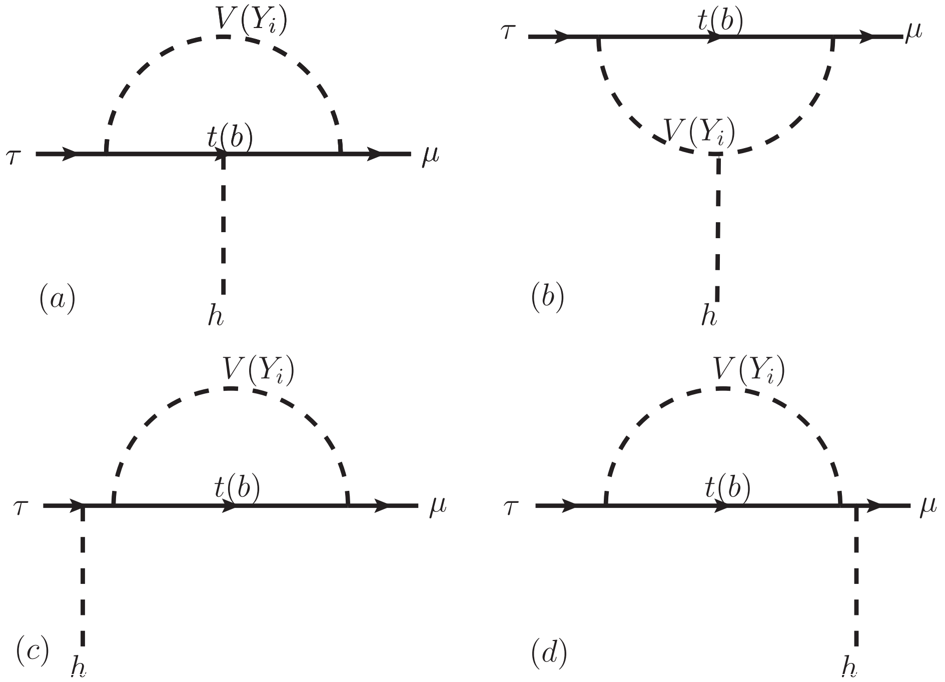

FIG. 4: Feynman diagrams of one-loop correction for $H^0-\mu-\tau$ vertex.

$$-\lambda_d^{32*}\lambda_e^{33*}\frac{N_c m_b}{16\pi^2 v}\left\{\sum_{i=1}^{2}O_{2i}O_{1i}\Big[I_{abc}(0,s_i)+I_a(0,s_i)\Big]\right.$$
$$\left.-\sum_{i,j=1}^{2}O_{2i}O_{1j}(O^T\Lambda O)_{ji}\frac{v^2}{m_{Y_b}^2}I_{b2}(s_{ij},s_j)\right\}, \tag{IV.2}$$

$$C_L = -\lambda_e^{23}\lambda_u^{33}\frac{N_c m_t}{16\pi^2 v}\left[I_{acd}(r_t,r_h)+I_a(r_t,r_h)-\lambda_{HX}\frac{v^2}{m_V^2}I_b(r_t,r_h)\right]$$
$$-\lambda_e^{23}\lambda_d^{33}\frac{N_c m_b}{16\pi^2 v}\left\{\sum_{i=1}^{2}O_{2i}O_{1i}\Big[I_{abc}(0,s_i)+I_a(0,s_i)\Big]\right.$$
$$\left.-\sum_{i,j=1}^{2}O_{2i}O_{1j}(O^T\Lambda O)_{ji}\frac{v^2}{m_{Y_b}^2}I_{b2}(s_{ij},s_j)\right\}, \tag{IV.3}$$

with $r_t = m_t^2/m_V^2, r_h = m_h^2/m_V^2$, $s_i = m_h^2/m_{Y_i}^2$, $s_{ij} = m_{Y_i}^2/m_{Y_j}^2$, and

$$\Lambda \equiv \begin{pmatrix} \lambda_{HR} & \lambda_{\rm mix} \\ \lambda_{\rm mix} & \widetilde{\lambda}_{HR} \end{pmatrix}. \tag{IV.4}$$

Note that the coupling combinations, $\lambda_u^{32*}\lambda_e^{33*}$ and $\lambda_d^{32*}\lambda_e^{33*}$ in C_R; $\lambda_e^{23}\lambda_u^{33}$ and $\lambda_e^{23}\lambda_d^{33}$ in C_L, are also found in the terms in C_R^γ and C_L^γ for describing primary contributions to $\tau^-\to\mu^-\gamma$, respectively. But here, no sizable cancellation emerges between terms being proportional to m_t and m_b when we adjust parameters for realizing the cancellation in $\tau^- \to \mu^-\gamma$. We ignore the apparently irrelevant terms being proportional to m_τ or m_μ, which arise from chirality flips in the external lines. The loop functions are

$$\begin{aligned}
I_{acd}(r_t, r_h) &= -\frac{1}{2} - 2\int [dx] \log\Big[x_3 + (1-x_3)r_t - x_1x_2r_h - i\varepsilon\Big] \\
&\quad + \int_0^1 dx \log\Big[x + (1-x)r_t - i\varepsilon\Big], \\
I_a(r_t, r_h) &= \int [dx] \frac{x_1x_2r_h - r_t}{x_3 + (1-x_3)r_t - x_1x_2r_h}, \\
I_b(r_t, r_h) &= \int [dx] \frac{1}{1 - x_3 + x_3r_t - x_1x_2r_h}, \\
I_{b2}(s_{ij}, s_j) &= \int [dx] \frac{1}{x_1s_{ij} + x_2 - x_1x_2s_j}, \qquad \text{(IV.5)}
\end{aligned}$$

where $\int [dx] \equiv \int_0^1 dx_1 \int_0^1 dx_2 \int_0^1 dx_3\, \delta(1 - x_1 - x_2 - x_3)$ and ε represents an infinitesimal positive value.[4] The form of the partial width $\Gamma_{h\to\mu^-\tau^+}$ is described by use of the Wilson coefficient C_R and C_L in Eq. (IV.1) as

$$\Gamma_{h\to\mu^-\tau^+} = \frac{\bar{\beta}}{16\pi m_h}\left[\left(m_h^2 - m_\mu^2 - m_\tau^2\right)\left(|C_R|^2 + |C_L|^2\right) - 2m_\mu m_\tau\left(C_RC_L^* + C_LC_R^*\right)\right], \qquad \text{(IV.6)}$$

with the kinetic factor

$$\bar{\beta} = \sqrt{1 - \frac{2(m_\mu^2 + m_\tau^2)}{m_h^2} + \frac{(m_\mu^2 - m_\tau^2)^2}{m_h^4}}, \qquad \text{(IV.7)}$$

while that of the conjugated process $\Gamma_{h\to\mu^+\tau^-}$ is straightforwardly obtained by the replacements $C_R \to C_R^*$ and $C_L \to C_L^*$. The inclusive width $\Gamma_{h\to\mu\tau}$ is simply defined as

$$\Gamma_{h\to\mu\tau} = \Gamma_{h\to\mu^-\tau^+} + \Gamma_{h\to\mu^+\tau^-}. \qquad \text{(IV.8)}$$

We use the value $\Gamma_h^{\rm SM} = 4.07\,\text{MeV}$ in $m_h = 125\,\text{GeV}$ reported by the LHC Higgs Cross Section Working Group [43] for evaluating $\mathcal{B}(h \to \mu\tau)$ in our model.

In the following analysis, as we did in the $\tau^- \to \mu^-\gamma$ in Sec. III, we adopt the assumption of $C_L = 0$. Among many terms in (IV.2), the two terms in the first line, *i.e.*, the top-quark contribution in Fig. 4 (a) dominates and we ignore the bottom-quark contributions in the following numerical estimation. In Fig. 3, we show the 2σ range to explain the excess in

---

[4] When X is real, the relation $\log[X \pm i\varepsilon] = \log[|X|] \pm i\pi\theta(-X)$ with the Heaviside theta function θ is useful.

$h \to \mu\tau$ shown in Eq. (I.1) in $(m_V, \lambda_{\rm conv})$-plane, where $\lambda_{\rm conv} \equiv |\lambda_u^{32}\lambda_e^{33}|$. We set $\lambda_{HR} = 1$, which is the coupling of the subleading term in Eq. (IV.2) with the suppression factor v^2/m_V^2. Here, an upper limit on $\lambda_{\rm conv}$ is estimated as $(\lambda_u^{32}\lambda_e^{33})|_{\rm max} = ((\lambda_u^{32}/\lambda_d^{32})\lambda_d^{32}\lambda_e^{33})|_{\rm max} \simeq 0.25 \cdot 4\pi \cdot 4\pi \simeq 40$, where 0.25 means a typical maximal value of the ratio $(\lambda_u^{32}/\lambda_d^{32})$ shown in Fig. 2 (when m_V is multi TeV and $\sin\alpha_Y = 1/\sqrt{2}$), and 4π comes from perturbative regime in λ_d^{32} and λ_e^{33}.

Combining Fig. 2 and Fig. 3, we can see that it is possible to explain the excess shown in Eq. (I.1) in our scenario. At first, we will remember the relation in the LQ's masses, $m_{Y_i} \sim m_V/6$ for ensuring natural cancellations between λ_u^{32} and λ_d^{32} in $\tau^- \to \mu^-\gamma$. When we request the (exact) cancellation in $\tau^- \to \mu^-\gamma$, as shown in Fig. 2, the ratio $(\lambda_u^{32}/\lambda_d^{32})^*$ should be smaller than unity. Considering a typical scale of m_V is more than a few TeV through the relation $m_{Y_i} \sim m_V/6$ and the latest LHC bounds on $m_{\rm LQ}$, as a rough estimation, $\lambda_{\rm conv}$ needs to be larger than around ten. Taking into account the bound via perturbativity $\lambda_e^{33} < 4\pi$, roughly speaking, λ_u^{32} should be greater than one through the definition of $\lambda_{\rm conv}$. Following this property, we should think about the property of the ratio $(\lambda_u^{32}/\lambda_d^{32})^*$. Roughly, greater than 0.1 is required for realizing the above inequality $\lambda_u^{32} > 1$ within the region where λ_d^{32} is still perturbative ($\lambda_d^{32} < 4\pi$). This means that the mixing angle α_Y should be large to some extent since when α_Y becomes far from the maximal case, the region with $(\lambda_u^{32}/\lambda_d^{32})^* > 0.1$ shrinks or disappears.[5]

As an example, we can satisfy $\tau^- \to \mu^-\gamma$ constraint, with $(m_V, m_{Y_1}, m_{Y_2}) = (3.6, 0.9, 0.6)$ TeV and $\sin\alpha_Y = 1/\sqrt{2}$ leading to $\lambda_u^{32}/\lambda_d^{32} \approx 0.15$. If we take $\lambda_d^{32} \approx 10$ and $\lambda_e^{33} \approx 4$, we get $\lambda_{\rm conv} \approx 6$, which can explain the central value shown in Eq. (I.1).

V. $(g-2)_\mu$

The anomalous magnetic moment of the muon has been measured to 0.5 ppm level [44],

$$a_\mu^{\rm exp} = 116\,592\,080(63) \times 10^{-11}. \tag{V.1}$$

---

[5] It is possible to modify the mass relation $m_{Y_i} \sim m_V/6$ without caring about the difference between λ_u^{32} and λ_d^{32}. When m_V is heavier than the case following $m_{Y_i} \sim m_V/6$, the top contribution in $\tau^- \to \mu^-\gamma$ decreases and the ratio $(\lambda_u^{32}/\lambda_d^{32})^*$ can get to be large, which means that larger λ_u^{32} would be realizable. On the other hand, however, a large m_V suppresses the process $h \to \mu\tau$.

Theoretical calculation in the SM has similar precision [45]

$$a_\mu^{\rm SM} = 116\,591\,785(61) \times 10^{-11}. \tag{V.2}$$

The discrepancy

$$\Delta a_\mu = a_\mu^{\rm exp} - a_\mu^{\rm SM} = (295 \pm 88) \times 10^{-11} \tag{V.3}$$

is believed to come from new physics contributions.

However, we should also keep in mind that there is a possibility that the discrepancy (or part of it) comes from underestimated uncertainties in hadronic part, for example, in hadronic light-by-light scattering. Lattice calculations [46–48] as well as calculations using dispersion relations [49–51] will reduce the hadronic uncertainties in the future.

In our model the leptoquark contribution to $(g-2)_\mu$ is given by

$$\begin{aligned}\Delta a_\mu \;=&\; -\frac{N_c m_\mu}{8\pi^2 m_V^2}\left[m_\mu\Big(\big|\lambda_e^{23}\big|^2 + \big|\lambda_u^{32}\big|^2\Big)\Big(\frac{2}{3}I_1(x) + \frac{5}{3}J_1(x)\Big) + {\rm Re}(\lambda_u^{32}\lambda_e^{23})m_t\Big(\frac{2}{3}I_2(x) + \frac{5}{3}J_2(x)\Big)\right]\\ &- \sum_{j=1,2}\frac{N_c m_\mu}{8\pi^2 m_{Y_j}^2}\left[m_\mu\Big(\big|\lambda_e^{23}\big|^2 O_{1j}^2 + \big|\lambda_d^{32}\big|^2 O_{2j}^2\Big)\Big(-\frac{1}{3}I_1(y_j) + \frac{2}{3}J_1(y_j)\Big)\right.\\ &+\left. {\rm Re}(\lambda_d^{32}\lambda_e^{23})O_{1j}O_{2j}m_b\Big(-\frac{1}{3}I_2(y_j) + \frac{2}{3}J_2(y_j)\Big)\right],\end{aligned} \tag{V.4}$$

the loop functions are given in (III.3). We notice that, if we set $m_{\mu,\tau} \to 0$ in C_R^γ in Eq. (III.2) and inside the square brackets in Δa_μ in Eq. (V.4), Δa_μ is exactly proportional to C_R^γ as

$$\Delta a_\mu = -\frac{4m_\mu}{e}\frac{\lambda_e^{23}}{\lambda_e^{33}}C_R^\gamma, \tag{V.5}$$

where we assumed all the couplings are real. If we use the current upper bound of C_R^γ in (III.6), we get

$$\Delta a_\mu \approx -(66.3 \times 10^{-11})\frac{\lambda_e^{23}}{\lambda_e^{33}}. \tag{V.6}$$

Therefore we see that, if $-7 \lesssim \lambda_e^{23}/\lambda_e^{33} \lesssim -2$, we can explain the muon $(g-2)_\mu$ with $\pm 2\sigma$ accuracy.

Since in our case the Yukawa couplings to explain $h \to \mu\tau$ and $(g-2)_\mu$ are rather large, one may expect higher order diagrams such as Barr-Zee type two-loop diagrams [52] may enhance $(g-2)_\mu$ as in the case of MSSM with large $\tan\beta$ [53, 54]. In our estimate, the

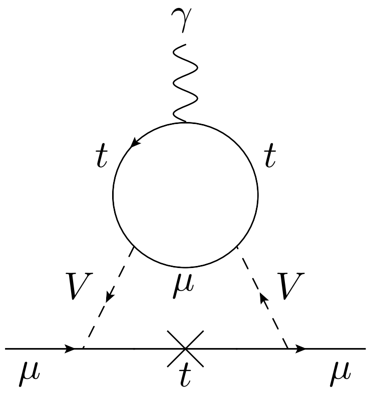

FIG. 5: A two-loop Barr-Zee type diagram for $(g-2)_\mu$.

dominant two-loop diagram is shown in Fig. 5. Other diagrams, such as the one with LQs running inside the loop, are suppressed, for example, by small muon mass, and we do not consider them. Although the diagram in Fig. 5 may look comparable with the one-loop diagrams due to large $\lambda_u^{32}\lambda_e^{23}$, we still need chirality flip inside the muon line in the fermionic triangle loop. Concretely, the diagram is estimated to be suppressed at least by

$$\sim \frac{1}{16\pi^2}\lambda_u^{32}\lambda_e^{33}\frac{m_\mu}{m_t} \sim 10^{-3} \tag{V.7}$$

compared to the one-loop diagram.

VI. CONCLUSION

In this paper, we considered the recent CMS excess in $h \to \mu\tau$ and the muon $(g-2)$ anomaly. We showed that we can accommodate both discrepancies by introducing two leptoquarks $R_2(3,2,7/6)$ and $\widetilde{R}_2(3,2,1/6)$ that are free from proton decay problems at renormalizable level. The constraints from lepton flavor violating process $\tau^- \to \mu^-\gamma$ can be evaded by a natural cancellation between leptoquark contributions with some tuning on λ_u^{32} and λ_d^{32}, where their orders can be the same. When the cancellation is realized, sizable couplings contributing to $h \to \mu\tau$ are allowed and then we give a reasonable explanation on the excess. The $(g-2)_\mu$ anomaly is also explained. Finally, we mention that various kinds of other anomalies in flavor physics have been reported [55–60]. Giving a more exhaustive explanation in the context of leptoquarks would be an important task [61].

Acknowledgments

K.N. is grateful to Tomohiro Abe, Shinya Kanemura, Kin-ya Oda, Makoto Sakamoto and Koji Tsumura for fruitful discussions. This work is supported in part by National Research Foundation of Korea (NRF) Research Grant No. NRF-2015R1A2A1A05001869 (S.B.).

[1] W. Buchmuller, R. Ruckl and D. Wyler, Phys. Lett. B **191** (1987) 442 [Phys. Lett. B **448** (1999) 320].
[2] G. Aad *et al.* [ATLAS Collaboration], arXiv:1508.04735 [hep-ex].
[3] V. Khachatryan *et al.* [CMS Collaboration], Phys. Lett. B **739**, 229 (2014) [arXiv:1408.0806 [hep-ex]].
[4] V. Khachatryan *et al.* [CMS Collaboration], JHEP **1507**, 042 (2015) [arXiv:1503.09049 [hep-ex]].
[5] CMS Collaboration, Report No. PAS EXO-12-041, http://cds.cern.ch/record/1742179/files/.
[6] F. S. Queiroz, K. Sinha and A. Strumia, Phys. Rev. D **91** (2015) 3, 035006 [arXiv:1409.6301 [hep-ph]].
[7] V. Khachatryan *et al.* [CMS Collaboration], Phys. Lett. B **749**, 337 (2015) [arXiv:1502.07400 [hep-ex]].
[8] G. Aad *et al.* [ATLAS Collaboration], arXiv:1508.03372 [hep-ex].
[9] G. Blankenburg, J. Ellis and G. Isidori, Phys. Lett. B **712** (2012) 386 [arXiv:1202.5704 [hep-ph]].
[10] R. Harnik, J. Kopp and J. Zupan, JHEP **1303** (2013) 026 [arXiv:1209.1397 [hep-ph]].
[11] S. Davidson and P. Verdier, Phys. Rev. D **86** (2012) 111701 [arXiv:1211.1248 [hep-ph]].
[12] J. Kopp and M. Nardecchia, JHEP **1410** (2014) 156 [arXiv:1406.5303 [hep-ph]].
[13] A. Celis, V. Cirigliano and E. Passemar, arXiv:1409.4439 [hep-ph].
[14] C. J. Lee and J. Tandean, JHEP **1504**, 174 (2015) [arXiv:1410.6803 [hep-ph]].
[15] L. de Lima, C. S. Machado, R. D. Matheus and L. A. F. do Prado, arXiv:1501.06923 [hep-ph].
[16] I. de Medeiros Varzielas and G. Hiller, JHEP **1506**, 072 (2015) [arXiv:1503.01084 [hep-ph]].
[17] B. Bhattacherjee, S. Chakraborty and S. Mukherjee, arXiv:1505.02688 [hep-ph].
[18] Y. n. Mao and S. h. Zhu, arXiv:1505.07668 [hep-ph].

[19] X. G. He, J. Tandean and Y. J. Zheng, JHEP **1509**, 093 (2015) [arXiv:1507.02673 [hep-ph]].

[20] T. Goto, R. Kitano and S. Mori, arXiv:1507.03234 [hep-ph].

[21] W. Altmannshofer, S. Gori, A. L. Kagan, L. Silvestrini and J. Zupan, arXiv:1507.07927 [hep-ph].

[22] A. Pilaftsis, Phys. Lett. B **285**, 68 (1992).

[23] A. Arhrib, Y. Cheng and O. C. W. Kong, Europhys. Lett. **101** (2013) 31003 [arXiv:1208.4669 [hep-ph]].

[24] A. Falkowski, D. M. Straub and A. Vicente, JHEP **1405** (2014) 092 [arXiv:1312.5329 [hep-ph]].

[25] A. Dery, A. Efrati, Y. Nir, Y. Soreq and V. Susič, Phys. Rev. D **90** (2014) 115022 [arXiv:1408.1371 [hep-ph]].

[26] M. D. Campos, A. E. C. Hernández, H. Päs and E. Schumacher, Phys. Rev. D **91** (2015) 11, 116011 [arXiv:1408.1652 [hep-ph]].

[27] D. Aristizabal Sierra and A. Vicente, Phys. Rev. D **90** (2014) 11, 115004 [arXiv:1409.7690 [hep-ph]].

[28] J. Heeck, M. Holthausen, W. Rodejohann and Y. Shimizu, Nucl. Phys. B **896**, 281 (2015) [arXiv:1412.3671 [hep-ph]].

[29] A. Crivellin, G. D'Ambrosio and J. Heeck, Phys. Rev. Lett. **114**, 151801 (2015) [arXiv:1501.00993 [hep-ph]].

[30] I. Doršner, S. Fajfer, A. Greljo, J. F. Kamenik, N. Košnik and I. Nišandžic, JHEP **1506** (2015) 108 [arXiv:1502.07784 [hep-ph]].

[31] Y. Omura, E. Senaha and K. Tobe, JHEP **1505**, 028 (2015) [arXiv:1502.07824 [hep-ph]].

[32] A. Crivellin, G. D'Ambrosio and J. Heeck, Phys. Rev. D **91**, no. 7, 075006 (2015) [arXiv:1503.03477 [hep-ph]].

[33] D. Das and A. Kundu, Phys. Rev. D **92**, no. 1, 015009 (2015) [arXiv:1504.01125 [hep-ph]].

[34] C. W. Chiang, H. Fukuda, M. Takeuchi and T. T. Yanagida, arXiv:1507.04354 [hep-ph].

[35] A. Crivellin, J. Heeck and P. Stoffer, arXiv:1507.07567 [hep-ph].

[36] K. Cheung, W. Y. Keung and P. Y. Tseng, arXiv:1508.01897 [hep-ph].

[37] F. J. Botella, G. C. Branco, M. Nebot and M. N. Rebelo, arXiv:1508.05101 [hep-ph].

[38] S. Baek and Z. F. Kang, arXiv:1510.00100 [hep-ph].

[39] F. Jegerlehner and A. Nyffeler, Phys. Rept. **477** (2009) 1 [arXiv:0902.3360 [hep-ph]].

[40] M. Benayoun, P. David, L. DelBuono and F. Jegerlehner, Eur. Phys. J. C **73** (2013) 2453

[arXiv:1210.7184 [hep-ph]].

[41] J. M. Arnold, B. Fornal and M. B. Wise, Phys. Rev. D **88**, 035009 (2013) [arXiv:1304.6119 [hep-ph]].

[42] B. Aubert *et al.* [BaBar Collaboration], Phys. Rev. Lett. **104**, 021802 (2010) [arXiv:0908.2381 [hep-ex]].

[43] S. Heinemeyer *et al.* [LHC Higgs Cross Section Working Group Collaboration], arXiv:1307.1347 [hep-ph].

[44] G. W. Bennett *et al.* [Muon g-2 Collaboration], Phys. Rev. Lett. **92** (2004) 161802 [hep-ex/0401008].

[45] J. P. Miller, E. de Rafael and B. L. Roberts, Rept. Prog. Phys. **70** (2007) 795 [hep-ph/0703049].

[46] T. Blum, S. Chowdhury, M. Hayakawa and T. Izubuchi, Phys. Rev. Lett. **114**, no. 1, 012001 (2015) doi:10.1103/PhysRevLett.114.012001 [arXiv:1407.2923 [hep-lat]].

[47] T. Blum, N. Christ, M. Hayakawa, T. Izubuchi, L. Jin and C. Lehner, arXiv:1510.07100 [hep-lat].

[48] J. Green, N. Asmussen, O. Gryniuk, G. von Hippel, H. B. Meyer, A. Nyffeler and V. Pascalutsa, arXiv:1510.08384 [hep-lat].

[49] G. Colangelo, M. Hoferichter, M. Procura and P. Stoffer, JHEP **1409**, 091 (2014) doi:10.1007/JHEP09(2014)091 [arXiv:1402.7081 [hep-ph]].

[50] V. Pauk and M. Vanderhaeghen, Phys. Rev. D **90**, no. 11, 113012 (2014) doi:10.1103/PhysRevD.90.113012 [arXiv:1409.0819 [hep-ph]].

[51] G. Colangelo, M. Hoferichter, M. Procura and P. Stoffer, JHEP **1509**, 074 (2015) doi:10.1007/JHEP09(2015)074 [arXiv:1506.01386 [hep-ph]].

[52] S. M. Barr and A. Zee, Phys. Rev. Lett. **65**, 21 (1990) [Phys. Rev. Lett. **65**, 2920 (1990)]. doi:10.1103/PhysRevLett.65.21

[53] A. Arhrib and S. Baek, Phys. Rev. D **65**, 075002 (2002) doi:10.1103/PhysRevD.65.075002 [hep-ph/0104225].

[54] S. Baek, Phys. Lett. B **595**, 461 (2004) doi:10.1016/j.physletb.2004.05.071 [hep-ph/0406007].

[55] J. P. Lees *et al.* [BaBar Collaboration], Phys. Rev. Lett. **109** (2012) 101802 [arXiv:1205.5442 [hep-ex]].

[56] J. P. Lees *et al.* [BaBar Collaboration], Phys. Rev. D **88** (2013) 7, 072012 [arXiv:1303.0571 [hep-ex]].

[57] R. Aaij *et al.* [LHCb Collaboration], Phys. Rev. Lett. **111** (2013) 191801 [arXiv:1308.1707 [hep-ex]].

[58] R. Aaij *et al.* [LHCb Collaboration], Phys. Rev. Lett. **113** (2014) 151601 [arXiv:1406.6482 [hep-ex]].

[59] R. Aaij *et al.* [LHCb Collaboration], arXiv:1506.08614 [hep-ex].

[60] M. Huschle *et al.* [Belle Collaboration], arXiv:1507.03233 [hep-ex].

[61] S. Baek and K. Nishiwaki, work in progress.